

NASA Technical Memorandum 87597

# Application of Mathematical Optimization Procedures to a Structural Model of a Large Finite-Element Wing

FOR REFERENCE  
NOT TO BE TAKEN FROM THIS ROOM

Joanne L. Walsh

JANUARY 1986

LIBRARY COPY

MAIL ROOM CENTER  
LINDSEY BLDG  
HAMPTON, VIRGINIA





NASA Technical Memorandum 87597

Application of Mathematical  
Optimization Procedures to  
a Structural Model of a  
Large Finite-Element Wing

Joanne L. Walsh  
*Langley Research Center*  
*Hampton, Virginia*

**NASA**  
National Aeronautics  
and Space Administration  
**Scientific and Technical  
Information Branch**

1986



## INTRODUCTION

To date, few applications have been presented of formal mathematical programming optimization procedures to large finite-element structural models. The use of formal optimization procedures for airplane wing design is reviewed by Ashley in reference 1. This review indicates that most optimization applications use simplified structural models of wings (e.g., rectangular cantilever wing boxes), although a few exceptions are found. Some applications included in reference 1 are a conceptual arrow-wing supersonic transport optimized for flutter constraints and a Mirage delta wing optimized for static and aeroelastic constraints. The preliminary design of an advanced transport wing subject to strength, stiffness, and aeroelastic constraints is described in references 2 and 3. The aeroelastic optimization of a fighter wing is described in reference 4. Optimization of a conceptual model of a supersonic transport wing for minimum structural mass is described in reference 5.

An effort is underway at the NASA Langley Research Center to demonstrate the use of formal mathematical programming procedures for the design of realistic airplane wings to achieve maximum fuel efficiency (ref. 6). The focus of a cooperative effort between NASA and the Lockheed-California Company is to perform design studies on the wing of an L-1011 derivative airplane by using two different approaches. Lockheed is using a traditional method of design involving parametric studies, whereas NASA is applying formal optimization procedures as described in reference 6. The purpose of the work described in this paper is to advance one step toward a formal structural optimization system that will eventually be suitable for the detailed design of an airplane wing.

The optimization analysis system described in the present work is denoted as "OPTREAL" and uses the general-purpose finite-element analysis program (ref. 7) known as Engineering Analysis Language (EAL) to perform the structural analysis and to calculate structural sensitivity derivatives. The general-purpose optimization program CONMIN (ref. 8), which is a FORTRAN program for constrained function minimization, is used to minimize an objective function that is subject to a set of inequality constraints by employing a usable-feasible directions search algorithm. The optimization process requires many evaluations of the objective function and constraints before the optimum design is obtained. This process can be very expensive if full analyses are made for each function evaluation. However, as Miura points out in reference 9, the optimization process primarily uses analysis results to move in the direction of the optimum design; therefore, a full analysis needs to be made only occasionally during the design process and always at the end to check the final design. Thus, various approximation techniques can be used during the optimization to reduce costs. In the present work, the objective function and constraints are approximated using a piecewise linear analysis that consists of linear Taylor series expansions for the objective function and the constraints based on the values for the design variables from CONMIN and static analysis and sensitivity information from EAL analyses.

This paper describes the optimization system and its application to a minimum mass optimization of a large transport-type wing designed to satisfy stress constraints while subjected to two static loading conditions. Results obtained from using the system are also compared with results obtained from using a fully stressed design procedure. Details of the optimization system are given in the appendix.

## SYMBOLS AND ABBREVIATIONS

$A_z$	cross-sectional area of stiffener (fig. 5)
$b$	stiffener spacing (fig. 5)
$C_{ij}$	constitutive matrix component (eq. (24))
$E$	modulus of elasticity
$F$	objective function
$\{f\}$	applied load vector
$g$	inequality constraints
$[K]$	stiffness matrix
$N_x$	inplane stress resultant, x-direction
$N_{xy}$	inplane shear stress resultant
$N_y$	inplane stress resultant, y-direction
$[S]$	stress displacement matrix
$T_1$	skin thickness (fig. 5)
$T_2$	equivalent smeared thickness of stiffener (fig. 5)
$\{u\}$	displacement vector
$V_k$	kth design variable
$\Delta V_k$	kth design variable increment
$\{V\}$	vector of independent design variables
$v_i$	ith dependent design variable
$\{v\}$	vector of dependent design variables
$x, y, z$	Cartesian coordinates
$\beta$	nondimensional parameter representing location along wing span (fig. 4)
$\gamma_{xy}$	engineering shear strain
$\delta$	move limit
$\epsilon_x$	membrane strain in x-direction
$\epsilon_y$	membrane strain in y-direction
$\nu$	Poisson's ratio

$\sigma_a$  allowable stress  
 $\bar{\sigma}$  Von Mises stress (eq. (8))  
 $\{\sigma\}$  stress vector

Subscripts:

$i, k$  design variable numbers  
 $l$  lower  
 $o$  original (unperturbed)  
 $u$  upper  
 $1$  skin  
 $2$  stiffener

Superscripts:

$n$  new (perturbed)  
 $o$  original (unperturbed)

Abbreviations:

FSD fully stressed design  
NDV number of design variables

### OPTIMIZATION PROCEDURES

The use of a formal mathematical programming procedure requires the specification of an objective function  $F(V)$  that is the quantity to be minimized, a set of design variables  $V$  that are the quantities which are changed in order to minimize the objective function, and a set of inequality constraints  $g$  that are requirements which must be satisfied (e.g., stresses within acceptable limits). The optimization problem can be stated as follows:

Find the set of variables  $V$  such that

$$F(V) \rightarrow \text{Minimum}$$

subject to

$$g \leq 0 \tag{1}$$

## Optimization Algorithm

The basic optimization algorithm used in this study is a combination of the optimization program CONMIN (ref. 8) and a piecewise linear approximation. Both are discussed in this section.

CONMIN.- CONMIN is a general-purpose optimization program that performs constrained minimization using a usable-feasible directions search algorithm. In the search for new design variable values, CONMIN requires derivatives of the objective function and constraints. The user has the option of either letting CONMIN determine the derivatives by finite differences or supplying derivative information to CONMIN. The latter method will be used herein.

Piecewise linear approximation.- Since structural analyses using large finite-element models are computationally expensive and time-consuming, approximate analysis methods are employed to reduce time and computer costs. In these approximate analysis methods, previously calculated derivatives of the objective function and constraint functions with respect to the design variables are used for linear extrapolation of these functions. The assumption of linearity is valid over a suitably small interval of the design variable values and will not introduce a large error into the analysis provided the interval remains sufficiently small. This approximate analysis will be referred to as a "piecewise linear approximation."

Specifically, the objective function  $F$ , the constraints  $g$ , and their respective derivatives are calculated for the design variables  $V$  using a full EAL analysis. A first-order Taylor series expansion, which approximates the new objective function and the constraint values based on values for the design variables obtained from CONMIN, is given as follows:

$$F = F_0 + \sum_{k=1}^{NDV} \frac{\partial F}{\partial v_k} (v_k - v_{0,k}) \quad (2)$$

and

$$g = g_0 + \sum_{k=1}^{NDV} \frac{\partial g}{\partial v_k} (v_k - v_{0,k}) \quad (3)$$

where  $NDV$  is the number of design variables,  $F$  is the extrapolated value of the objective function,  $g$  is the extrapolated value of the constraint, and  $v_k$  is the design variable value obtained from CONMIN. The symbols  $F_0$ ,  $g_0$ , and  $v_{0,k}$  are the values for the objective function, constraints, and design variables, respectively, from the full analysis.

The use of the piecewise linear approach requires that limits be imposed on the design variable changes (referred to as "move limits") to control the errors introduced by the linearity assumption. A move limit is specified as an increment  $\delta$ . (For this work,  $\delta = 0.1$ .) These upper and lower move limits result in two additional constraints on each of the design variables. The move limits are formulated

as two constraints so that the proper derivatives of the constraints are obtained. These constraints are formulated in the following manner:

$$\left. \begin{aligned} g_u &= V_k - V_{k,u} \\ g_l &= V_{k,l} - V_k \end{aligned} \right\} \quad (4a)$$

where  $V_{k,u}$  and  $V_{k,l}$  are the upper and lower bounds on the kth design variable, respectively, and are given by

$$\left. \begin{aligned} V_{k,u} &= V_k^o + \delta \\ V_{k,l} &= V_k^o - \delta \end{aligned} \right\} \quad (4b)$$

where  $\delta$  is the move limit and  $V_k^o$  is the unperturbed value of the kth design variable (i.e., the design variable value used in the structural analysis). The move limit constraints are formulated by combining equations (4a) and (4b) and nondimensionalizing. Thus,

$$g_u = \frac{V_k - V_k^o}{\delta} - 1 \quad (5a)$$

and

$$g_l = \frac{V_k^o - V_k}{\delta} - 1 \quad (5b)$$

#### Objective Function

In a minimum mass-strength optimization problem, the objective is to find the distribution of structural material in the wing that has the least mass while satisfying requirements on stresses in the wing skin. Thus, the objective function (eq. (1)) is defined as follows:

$$F(V) = \text{Mass} \quad (6)$$

## Design Variables

For this study the design variables  $V$  are the coefficients in a polynomial expression that describes the skin thickness distribution in the wing. Using the coefficients of the polynomial as design variables allows the specification of a large number of finite-element thicknesses by a few parameters.

## Constraints

Two types of constraints are used in this study. One is a stress constraint that requires that the Von Mises stress  $\bar{\sigma}$  in each wing cover panel be less than a given allowable value  $\sigma_a$ ; i.e.,

$$g = \frac{\bar{\sigma}}{\sigma_a} - 1 \quad (7)$$

where  $\bar{\sigma}$  is the Von Mises stress defined as

$$\bar{\sigma} = (\sigma_x^2 + \sigma_y^2 - \sigma_x \sigma_y + 3\sigma_{xy}^2)^{1/2} \quad (8)$$

The second type of constraint is the move limit due to the piecewise linearity approximation used in the optimization procedure. These move limit constraints are defined by equations (5).

## Constraint Derivatives

The derivative of the stress constraint is found by differentiating equation (7) with respect to the  $k$ th design variable  $V_k$ . Thus,

$$\frac{\partial g}{\partial V_k} = \frac{1}{\sigma_a} \frac{\partial \bar{\sigma}}{\partial V_k} \quad (9)$$

where  $\partial \bar{\sigma} / \partial V_k$  is the stress derivative. The calculation of the stress  $\bar{\sigma}$  and the stress derivative will be discussed in the next section. The derivatives of the move limit constraints with respect to the  $k$ th design variable  $V_k$  are found by differentiating equations (5). Thus,

$$\frac{\partial g_u}{\partial V_k} = \frac{1}{\delta} \quad (10)$$

and

$$\frac{\partial g_l}{\partial v_k} = - \frac{1}{\delta} \quad (11)$$

where  $\delta$  is the move limit.

## STRUCTURAL RESPONSE AND SENSITIVITY CALCULATIONS

### Structural Analysis

The basic structural analysis program used in the system is a general-purpose finite-element analysis system (ref. 7) known as Engineering Analysis Language (EAL). The EAL program is a modular system of independent processors that are called using a high-level command language in user-created "runstreams" (analogous to calling subroutines in FORTRAN). These runstreams can be created and used for a variety of purposes such as repetitive analyses. EAL also provides for the incorporation of user-developed FORTRAN subroutines as external EAL processors. EAL and its capabilities will be discussed in further detail in the appendix.

### Sensitivity Analysis

The optimization system requires the calculation of sensitivity derivatives. The basic methodology for implementing structural sensitivity derivative calculations into a general-purpose finite-element analysis system (ref. 10) is described in reference 11. Further development and incorporation of this methodology in EAL as runstreams is described in reference 12. In the present system the runstreams of reference 12 are used for the sensitivity derivatives. The stress and displacement derivatives with respect to the design variables are obtained using the semianalytical approach described in reference 12. The semianalytical approach uses an analytical expression for the displacement derivatives combined with a finite-difference approximation for the derivative of the stiffness matrix as outlined below.

Equations for the structural sensitivity derivatives are based on the equilibrium equations for linear static structural analysis

$$[K]\{u\} = \{f\} \quad (12)$$

where  $[K]$  is the linear stiffness matrix,  $\{u\}$  is the vector of nodal displacements, and  $\{f\}$  is the applied load vector. Element stresses  $\{\sigma\}$  are related to the nodal displacements by

$$\{\sigma\} = [S]\{u\} \quad (13)$$

where  $[S]$  is defined as the stress displacement matrix (ref. 12).

Displacement derivatives.- The displacement derivatives are calculated by differentiating equation (12) with respect to each design variable. Assuming that the applied load vector  $\{f\}$  is independent of the design variables, then

$$[K] \frac{\partial \{u\}}{\partial v_k} = - \frac{\partial [K]}{\partial v_k} \{u\} \quad (14)$$

where the derivative of the stiffness matrix with respect to the  $k$ th design variable  $\partial[K]/\partial v_k$  is calculated by using a forward finite-difference approximation

$$\frac{\partial [K]}{\partial v_k} \approx \frac{\Delta [K]}{\Delta v_k} \approx \frac{[K]^n - [K]^o}{v_k^n - v_k^o} \quad (15)$$

and  $[K]^n$  is the perturbed stiffness matrix formed by incrementing the  $k$ th design variable by  $\Delta v_k$ ; i.e.,

$$v_k^n = v_k^o + \Delta v_k \quad (16)$$

and  $[K]^o$  and  $v_k^o$  are the original (unperturbed) stiffness matrix and the unperturbed  $k$ th design variable, respectively. The displacement derivative  $\partial\{u\}/\partial v_k$  in equation (14) is computed using the factored stiffness matrix from the solution of equation (12).

Stress derivatives.- The stress derivative  $\partial\{\sigma\}/\partial v_k$  is found by first approximating the perturbed displacement vector  $\{u\}_k^n$  by a first-order Taylor series expansion

$$\{u\}_k^n = \{u\}^o + \frac{\partial \{u\}}{\partial v_k} (v_k^n - v_k^o) \quad (17)$$

where  $\partial\{u\}/\partial v_k$  is calculated from equation (14),  $v_k^n$  is calculated by equation (16), and  $\{u\}^o$  and  $v_k^o$  are the unperturbed displacement and the  $k$ th unperturbed independent design variable, respectively. Using equation (13), the  $k$ th perturbed stress vector  $\{\sigma\}_k^n$  is given by

$$\{\sigma\}_k^n = [S]_k^n \{u\}_k^n \quad (18)$$

and the kth stress derivative is calculated by using a forward finite-difference approximation

$$\frac{\partial \{\sigma\}}{\partial v_k} \approx \frac{\{\sigma\}_k^n - \{\sigma\}^o}{v_k^n - v_k^o} \quad (19)$$

with  $\{\sigma\}^o$  given by equation (13). The derivative of the Von Mises stress (eq. (8)) is given by

$$\frac{\partial \bar{\sigma}}{\partial v_k} = \frac{\sigma_x \frac{\partial \sigma_x}{\partial v_k} + \sigma_y \frac{\partial \sigma_y}{\partial v_k} - \frac{1}{2} \left( \sigma_y \frac{\partial \sigma_x}{\partial v_k} + \sigma_x \frac{\partial \sigma_y}{\partial v_k} \right) + 3\sigma_{xy} \frac{\partial \sigma_{xy}}{\partial v_k}}{\bar{\sigma}} \quad (20)$$

where the derivatives of the stress components are given by equation (19) and  $\bar{\sigma}$  is given by equation (8).

## WING MODEL DESCRIPTION

The advanced transport airplane being studied in the cooperative agreement between NASA and the Lockheed-California Company (ref. 6) is illustrated in figure 1. The airplane is an L-1011 derivative that will have a stretched body, a new flight station, a new propulsion system, a smaller tail, and a new wing. These modifications are indicated by the shaded regions of the airplane. The optimization process described above was applied to a finite-element model of this wing for a minimum mass-strength study.

### Finite-Element Model

A NASTRAN finite-element model of the L-1011 transport airplane was developed at Lockheed (ref. 13) for use in their design procedure known as the Preliminary Aeroelastic Design of Structures (PADS). This NASTRAN finite-element model was converted to an EAL finite-element model for use in the present work.

The EAL finite-element model is shown in figure 2. The entire model of the airplane is shown in figure 2(a). The model of the wing is shown in figure 2(b). Since the focus of the study is on wing design, a detailed model is used for the wing structure and the wing-fuselage interface. The wing and wing-fuselage interface are modeled with rods and membrane elements. The fore and aft fuselage, the empennage, engine, and landing gear are modeled with beam elements. The resulting model (a symmetric half-model) has 641 nodes and 1749 elements. There are 170 beam elements (EAL element type E21) used to model the fuselage rings, fuselage beams, horizontal and vertical tails, the engine, the landing gear, the control-surface actuators, and the interface between the fuselage shell and beams. There are 775 bar elements (EAL element type E23) used to model the spar and rib caps and the stiffeners on the lower

fuselage shell. The wing centerbody interface, the fuselage-beam centerbody interface, and the actuator springs are modeled by 18 spring elements (EAL element type E25). The remainder of the model consists of 786 quadrilateral membrane elements (EAL element type E41) to model the wing cover skins, fuselage skin, wing rib and spar shear webs, and the aerodynamic pressure distribution panels.

Only the cover panels in the upper and lower surfaces of the main wing box are sized in the present study. Thus, of the 1749 elements in the finite-element model of the transport airplane, 216 elements (EAL element type E41) are to be sized. These elements are the wing cover panels in the upper and lower surfaces of the wing box and are shown in figure 3. The 108 elements in the upper wing box surface and the 108 elements in the lower wing box surface that are to be sized are shown in figures 3(a) and 3(b), respectively. The cover panels and stiffeners of the wing are made of aluminum with a modulus of elasticity of  $10.5 \times 10^6$  psi, a Poisson's ratio of 0.33, and a density of  $0.1 \text{ lbm/in}^3$ .

### Cover Panel Representation

The wing box is divided into two regions, inboard and outboard, with a rib near the engine pylon being the dividing line. (See fig. 4.) The wing is assumed to be symmetric so that the upper and lower surfaces have the same thickness distribution. The distribution of skin thickness  $T_1$  in the spanwise direction is described by a quadratic expression in a nondimensional parameter  $\beta$ , where  $\beta = 0$  at the airplane centerline,  $\beta = 0.12$  at the wing root, and  $\beta = 1.0$  at the wing tip (fig. 4). The skin thickness is assumed to be constant in the streamwise direction. The smeared stiffener thickness  $T_2$  is assumed to be proportional to the skin thickness  $T_1$ . There are two quadratic expressions used to describe the skin thickness distributions (one for each region of the wing) and two corresponding proportionality factors for the stiffener thickness distributions. For a given node point located at a nondimensional distance  $\beta$  from the wing centerline, the skin thickness and the stiffener thickness distributions are given by

$$\left. \begin{aligned} T_1 &= v_1 + v_2(1 - \beta) + v_3(1 - \beta)^2 \\ T_2 &= v_4 T_1 \end{aligned} \right\} \quad \text{(outboard)} \quad (21)$$

$$\left. \begin{aligned} T_1 &= v_5 + v_6(1 - \beta) + v_7(1 - \beta)^2 \\ T_2 &= v_8 T_1 \end{aligned} \right\} \quad \text{(inboard)} \quad (22)$$

Equations (21) and (22) contain eight undetermined coefficients,  $v_1$  to  $v_8$  that will be the design variables.

## Constitutive Properties of Wing Cover Panels

The EAL program requires a constitutive matrix for each element. For a membrane element, the constitutive matrix  $C$  relates the inplane stress resultants  $\{N\}$  to the membrane strains  $\{\epsilon\}$  in the following manner:

$$\begin{Bmatrix} N_x \\ N_y \\ N_{xy} \end{Bmatrix} = \begin{bmatrix} C_{11} & C_{12} & 0 \\ C_{12} & C_{22} & 0 \\ 0 & 0 & C_{33} \end{bmatrix} \begin{Bmatrix} \epsilon_x \\ \epsilon_y \\ \gamma_{xy} \end{Bmatrix} \quad (23)$$

In the wing model, two thicknesses (a skin thickness  $T_1$  and a stiffener thickness  $T_2$ ), two moduli of elasticity  $E_1$  and  $E_2$  (for this work,  $E_1 = E_2 = E$ ), and Poisson's ratio  $\nu$  are associated with each element in the wing box cover skin. An effective thickness and stiffness for each element are used to define the elements in equation (23). The effective thickness is determined by smearing the stiffener thickness and combining it with the skin thickness. The two thicknesses associated with each element are shown in figure 5. The nonzero elements in matrix  $C$  in equation (23) are given by

$$\left. \begin{aligned} C_{11} &= \frac{E_1 T_1 + E_2 T_2}{1 - \nu_{12} \nu_{21}} \\ C_{22} &= \frac{E_1 T_1}{1 - \nu_{12} \nu_{21}} \\ C_{12} &= \nu_{21} C_{11} \\ C_{33} &= \frac{E_1 T_1}{2(1 + \nu_{12})} \end{aligned} \right\} \quad (24)$$

where

$$\nu_{12} = \nu$$

and

$$\nu_{21} = \frac{E_1 T_1 \nu_{12}}{E_1 T_1 + E_2 T_2}$$

In the above equations,  $T_1$  and  $T_2$  are element centroidal thicknesses obtained by calculating the thicknesses  $T_1$  and  $T_2$  for each element node point from equations (21) and (22) and then taking an average of these node point thicknesses.

### Load Distributions

In the present work, two static load cases given in table I were used. The first load case represents a 50 000-lb force applied at the wing tip. The second case represents a distributed loading by 1000-lb forces applied at each node over the entire wing box. These two load cases result in 432 stress constraints (216 stress constraints for each load case).

## RESULTS AND DISCUSSION

### Overview

The optimization method has been applied to a minimum mass design of an L-1011 type of transport wing subject to stress constraints. The objective function reflects only the mass of the sized elements. A total of 448 constraints are used in this study (432 stress constraints and 16 move limit constraints on the design variables).

### Optimization Results

The starting values for the design variables are given in table II. The two coefficients  $V_4$  and  $V_8$  that determine the stiffener thicknesses were fixed at a value of 0.60 during the optimization process. (The ratio of the stiffener thickness to skin thickness is a constant in the existing L-1011 wing.) These values of the design variables result in a wing whose initial mass is 10 829 lb with 94 violated stress constraints.

The terms "cycle" (or outer loop) and "iteration" (or inner loop) will be used in the following discussion. The outer loop consists of structural analysis, derivative calculations, and a set of optimization calculations made in the inner loop. The inner loop consists of the optimization calculations within a given cycle to find an improved set of design variable values using a piecewise linear analysis based on the current set of derivatives.

A history of the objective function (mass of the sized cover panels) plotted against cycle number is shown in figure 6. In the figure each circular symbol represents a cycle. There are several optimization iterations between each symbol. On the first cycle the optimization process tries to eliminate the violated constraints and decrease the mass. However, because of the linearization approximation for the objective function and the constraint functions, using these design variable values obtained on cycle 1 results in 36 violated constraints when the structural analysis is performed at the beginning of cycle 2. This accounts for the increase in mass at the end of cycle 2 as CONMIN tries to eliminate the violated constraints. As shown in figure 6, since the value of the objective function does not change significantly after the 21st cycle, a "flat" minimum is indicated.

Histories of the design variables plotted against cycle number are shown in figure 7. All the design variables have converged after 30 cycles. The values for

the objective function and design variables for the final design (at 30 cycles) are given in table II. There are no violated constraints.

The effective thickness distribution (skin thickness plus smeared stiffener thickness) plotted against span location  $\beta$  is shown in figure 8. The effective thickness distributions for the initial and final cycles are shown in figure 8(a). These distributions, along with distributions from several intermediate cycles, are shown in figure 8(b). The initial thickness distribution is continuous (i.e., no gap between the inboard and outboard regions) and is nearly linear. As the optimization process proceeds, a gap at the 50-percent span location is present. The presence of this gap is due to two reasons. First, the expression for the thickness distribution is a low-order (quadratic) polynomial. If a higher-order polynomial were used, the polynomial would have more freedom to match thicknesses at the interface. Then, a better representation of the thickness distribution could be obtained. Second, the stress values for elements near the interface are low. If these were closer to being critical, the thicknesses from each region of the wing would approach each other and thus reduce the gap. A plot of the gap between the inboard and outboard thickness distributions at the 50-percent span location as a function of the number of cycles is shown in figure 9. The gap decreases with the number of cycles until the distributions cross over. After 30 cycles the growth in gap thickness has reached a constant value of about 0.05 in.

#### Comparison With Fully Stressed Design

The effective thickness distribution for the final design of the wing using OPTEAL is compared with the effective thickness distribution for the wing sized by using a fully stressed design (FSD) procedure. FSD is a procedure that can be useful for preliminary sizing of wings subject to stress and minimum gauge constraints. The FSD procedure sizes structural elements based on the ratio of calculated stress to allowable stress. As pointed out in reference 14, FSD is useful in obtaining low mass designs for nearly statically determinant structures, such as high-aspect-ratio wings like the one considered in the current work, but it can produce nonoptimum results for highly redundant structures. The FSD thickness distribution is obtained by calculating the thickness necessary for the wing box to be fully stressed at each of the 24 rib cross sections. The FSD results are based on simple beam theory and load case 1 only. The OPTEAL and FSD thickness distributions compared in figure 10 exhibit similar trends. At the tip the FSD thickness goes to 0 as the bending moment goes to 0 because minimum gauge is not considered. The quadratic thickness distribution used in OPTEAL is influenced by all the elements in the outboard region and does not go to 0 at the tip. The masses of the designs using the two approaches are within 10 percent. As shown in figure 11, the optimized wing has many elements that are nearly fully stressed. The stresses in the shaded, hatched, and cross-hatched elements in the upper wing surface (fig. 11(a)) and the lower wing surface (fig. 11(b)) are near the allowable stress value for load case 1, load case 2, and both load cases, respectively.

#### CONCLUDING REMARKS

Formal optimization procedures have been applied to a large finite-element model of a transport-airplane wing structure. The wing is designed for minimum mass subject to stress constraints for two load cases. The design variables are coefficients of polynomials describing the skin and stiffener thickness distributions. The skin distribution in the spanwise direction is described by two quadratic expressions (one

inboard and one outboard) and is constant in the streamwise direction. The stiffener thicknesses are proportional to the skin thickness.

An implementation of the procedure is developed that consists of the basic analysis and a sensitivity derivative capability in the finite-element analysis program for Engineering Analysis Language (EAL), a set of user-written FORTRAN processors, the general-purpose optimization program CONMIN, and a piecewise linear analysis. In the procedure, sensitivity derivatives are computed using a semianalytical method that combines finite-difference derivatives of the stiffness matrix with analytical expressions for the derivatives of the stresses and displacements.

Results are presented for a minimum mass design subject to stress requirements. The objective function, which is the mass in the wing cover panels, is found to have a "flat" minimum. Results obtained using the optimization analysis system (OPTEAL) compare favorably with those obtained using a fully stressed design procedure based on beam theory. The masses for the wing cover panels from the two procedures are within 10 percent.

NASA Langley Research Center  
Hampton, VA 23665-5225  
October 25, 1985

## APPENDIX

### OPTIMIZATION ANALYSIS SYSTEM (OPTEAL)

This section of the paper contains a description of the optimization analysis system denoted as "OPTEAL." First, the EAL program is described briefly. Next, a description of how EAL was integrated into the optimization system is given. Finally, a block diagram of the OPTEAL system is shown and discussed in detail.

### Engineering Analysis Language (EAL) System

A schematic of the EAL system configuration is shown in figure 12. EAL contains individual processors that communicate through a common data base consisting of one or more libraries of data sets. The data sets typically contain data describing the finite-element model of the structure (such as geometry) as well as response information that is accumulated during the execution of the processors. All data communication between processors is in terms of data sets. A set of data-handling utilities (ref. 15) transfers data between the processor in the central memory of the computer and the data base on auxiliary storage devices. The functions of the various EAL processors are shown in table III. The processors can be executed in any appropriate sequence, and a sequence of processor executions is denoted as a "runstream."

The EAL system also uses a set of flexible FORTRAN-like statements called executive control system (ECS) commands. A list of ECS commands is given in table 8-1 of reference 7. These commands allow branching, testing data, looping, and calling runstreams (similar to calling FORTRAN subroutines).

Besides the processors listed in table III, the EAL system also allows the user to write processors that can be executed in EAL. These user-written processors are known as external processors and are written in FORTRAN. Data are transferred between the data base and these external processors using the utilities described in reference 15. The processors also make use of the information stored in the individual data sets (ref. 16).

The EAL processors, with appropriate ECS commands organized as runstreams, are used to implement the analysis and derivative computations (eqs. (12) to (19)). These runstreams are based on those in the appendix of reference 12 with some modifications that will be discussed subsequently. The OPTEAL system combines those modified runstreams with three external processors called LINK, EPNG, and JOPT that are described subsequently.

### External Processor LINK

The processor LINK is an external EAL processor that updates the section properties table for the type E41 elements which are to be sized using equations (21) to (24). This processor utilizes information contained in the data base (node points, connectivities, design variable values, etc.) to update the section property table. This processor must be called once at the beginning of the analysis and then subsequently every time a design variable is changed. For example, if there are eight design variables, this processor must be executed nine times in the course of calculating derivatives. LINK enters the updated section properties into the EAL data base.

## External Processor EPNG

The processor EPNG is an external EAL processor that evaluates the constraints and the derivatives of the constraints for later use by the optimizer. EPNG first accesses the stress components computed by EAL and their derivatives computed by the method of reference 12 from the EAL data base. The processor then computes a Von Mises stress using equation (8) and uses equation (7) to obtain the corresponding constraint. Finally, derivatives of the stress constraints (eq. (7)) are calculated using equations (9) and (20).

## External Processor JOPT

The processor JOPT is an external EAL processor that contains the optimization program CONMIN (ref. 8) and the piecewise linear analysis. The role of JOPT is to find the values of the design variables that move toward a minimum value of the objective function while satisfying all the constraints. The piecewise linear analysis is used to extrapolate the objective function using equation (2) and the constraint equations using equation (3), which are then passed to the optimizer CONMIN that minimizes an objective function subject to inequality constraints. CONMIN uses a usable-feasible directions search algorithm to obtain new values for the design variables. New values for the objective function and constraints based on these new design variable values are extrapolated using the piecewise linear analysis. This process continues until the objective function has converged. Processor JOPT obtains all the CONMIN parameter values from the EAL data base. This processor also computes the additional constraints required for move limits and the derivatives of these constraints by the piecewise linear analysis. The constraints, move limits, and the derivatives of these constraints are given by equations (4), (5), (10), and (11).

## Organization of OPTEAL

The basic flow of information in OPTEAL is shown in the block diagram of figure 13. A detailed description of the process is given as follows:

### Block (1)

EAL data tables are set up initializing the CONMIN parameters (ref. 8). These tables will be accessed by the external processor JOPT. Although most of the parameter values will change depending on the problem, the one that will not change is NDFG, which is the finite-difference gradient option parameter in CONMIN. This parameter will always have the value of 1, which indicates that the user will supply all derivative information to CONMIN.

### Block (2)

The finite-element model of the wing is established. The node point locations, connectivities, element types (E23, E41, etc.), and section properties are defined. The elements to be sized are separated into four E41 groups: group 1 is the upper outboard surface; group 2 is the lower outboard surface; group 3 is the upper inboard surface; and group 4 is the lower inboard surface. The EAL processors TAB, ELD, and TAN are called and the EAL tables describing the loading on the wing are set up.

Block (3)

The EAL registers are initialized.

Block (4)

EAL tables containing initial values for the design variables are established. These are the values for the coefficients  $V_1$  to  $V_8$  in equations (21) and (22).

Block (5)

The wing symmetry condition (membrane (E41) thicknesses in the upper and lower wing surfaces are equal) is imposed using design variable linking. Specifically, group 1 thicknesses are the same as group 2, and group 3 thicknesses are the same as group 4.

Note in blocks (6) to (8): The external EAL processor LINK consists of blocks (6) to (8).

Block (6)

The skin and stiffener thicknesses at each node in the wing skin cover panels are computed using equations (21) and (22).

Block (7)

The effective thicknesses of the elements to be sized are computed as averages of the respective thicknesses of the four element node points.

Block (8)

The effective thicknesses of the elements are used in equations (24) to define the constitutive matrix  $C$  in equation (23). These matrix elements are used to update the EAL section properties table, which is then entered into the EAL data base using the utilities of reference 15.

Block (9)

The displacements  $\{u\}$  and the stresses  $\{\sigma\}$  in the sized wing cover skin elements (groups 1 to 4, type E41 elements) are calculated using equations (12) and (13).

Block (10)

The derivatives of the stiffness matrix are calculated by finite differences. A detailed description of this block is shown in figure 14.

#### Block (11)

After  $\partial[K]/\partial V$  has been computed, the derivatives of the displacements are computed from equation (14). Then, the derivatives of the stress components in the sized elements are found by using equation (19).

#### Block (12)

The external EAL processor EPNG is executed to extract the components of the stresses and their derivatives from the EAL data base to calculate the stress constraints (eqs. (7) and (8)) and the stress constraint derivatives (eqs. (19) and (20)). These values are entered into the EAL data base.

#### Block (13)

The objective function and its derivatives are calculated and entered into the EAL data base.

Note in blocks (14) to (16): The external EAL processor JOPT is executed.

#### Block (14)

The CONMIN parameter values, objective function, objective function derivatives, stress constraints, stress constraint derivatives, and design variable values are accessed from the EAL data base using the utilities of reference 15. The move limit constraints for the piecewise linear analysis are formed using equation (5). The derivatives of these constraints are found using equations (10) and (11).

#### Block (15)

The general-purpose optimization program CONMIN and the piecewise linear analysis are used to move toward the optimum values for the design variables. CONMIN uses derivatives and active constraints to determine a search direction toward a new set of design variables. The piecewise linear analysis is used to extrapolate values of the objective function and the constraints based on these new design variables.

#### Block (16)

The new set of design variables is entered into the EAL data base.

#### Block (17)

Convergence of the entire system is checked. If the mass of the wing has not changed by more than a specified tolerance over three consecutive cycles, it is assumed that convergence has occurred. Otherwise, control reverts back to block (6) and the procedure continues.

## REFERENCES

1. Ashley, Holt: On Making Things Best - Aeronautical Uses of Optimization. J. Aircr., vol. 19, no. 1, Jan. 1982, pp. 5-28.
2. Sobieszczanski, Jaroslaw; McCullers, L. Arnold; Ricketts, Rodney H.; Santoro, Nick J.; Beskenis, Sharon D.; and Kurtze, William L.: Structural Design Studies of a Supersonic Cruise Arrow Wing Configuration. Proceedings of the SCAR Conference - Part 2, NASA CP-001, [1977], pp. 659-683.
3. Sobieszczanski-Sobieski, Jaroslaw: An Integrated Computer Procedure for Sizing Composite Airframe Structures. NASA TP-1300, 1979.
4. Triplett, William E.: Aeroelastic Tailoring Studies in Fighter Aircraft Design. A Collection of Technical Papers on Structures - AIAA/ASME/ASCE/AHS 20th Structures, Structural Dynamics, and Materials Conference, Apr. 1979, pp. 72-78. (Available as AIAA Paper 79-0725.)
5. Rao, S. S.: Automated Optimum Design of Wing Structures - Deterministic and Probabilistic Approaches. NASA TM-84475, 1982.
6. Giles, Gary L.; and Wrenn, G. A.: Multidisciplinary Optimization Applied to a Transport Aircraft. Recent Experiences in Multidisciplinary Analysis and Optimization, Jaroslaw Sobieski, compiler, NASA CP-2327, Part 1, 1984, pp. 439-453.
7. Whetstone, W. D.: EISI-EAL Engineering Analysis Language Reference Manual - EISI-EAL System Level 2091. Engineering Information Systems, Inc., July 1983.
8. Vanderplaats, Garret N.: CONMIN - A FORTRAN Program for Constrained Function Minimization - User's Manual. NASA TM X-62282, 1973.
9. Miura, Hirokazu: Applications of Numerical Optimization Methods to Helicopter Design Problems: A Survey. NASA TM-86010, 1984.
10. Whetstone, W. D.: SPAR Structural Analysis System Reference Manual - System Level 13A. Volume I: Program Execution. NASA CR-158970-1, 1978.
11. Giles, Gary L.; and Rogers, James L., Jr.: Implementation of Structural Response Sensitivity Calculations in a Large-Scale Finite-Element Analysis System. A Collection of Technical Papers, Part 2: Structural Dynamics and Engineering - AIAA/ASME/ASCE/AHS 23rd Structures, Structural Dynamics and Materials Conference, May 1982, pp. 348-367. (Available as AIAA-82-0714.)
12. Camarda, Charles J.; and Adelman, Howard M.: Static and Dynamic Structural-Sensitivity Derivative Calculations in the Finite-Element-Based Engineering Analysis Language (EAL) System. NASA TM-85743, 1984.
13. Radovcich, N. A.: Preliminary Aeroelastic Design of Structures [PADS] Methods Development and Application. Aeroelastic Considerations in the Preliminary Design of Aircraft, AGARD-CP-354, Sept. 1983, pp. 1-1 - 1-29.
14. Adelman, Howard M.; Haftka, Raphael T.; and Tsach, Uri: Application of Fully Stressed Design Procedures to Redundant and Non-Isotropic Structures. NASA TM-81842, 1980.

15. Giles, Gary L.; and Haftka, Raphael T.: SPAR Data Handling Utilities.  
NASA TM-78701, 1978.
16. Cunningham, Sally W.: SPAR Data Set Contents. NASA TM-83181, 1981.

TABLE I.- WING LOADING

Load case	Joint number (see fig. 3)	$F_x$ , lb	$F_y$ , lb	$F_z$ , lb
1	5, 7, 9, 11, 13	0	0	10 000
2	5, 7, 9, 11, 13 23, 25, 27, 29, 31 41, 43, 45, 47, 49 . . . 437, 439, 441, 443, 445	0 ↓ ↓ ↓	0 ↓ ↓ ↓	1 000 ↓ ↓ ↓

TABLE II.- INITIAL AND FINAL DESIGN VARIABLE VALUES

Design variable	Initial value	Final value
$V_1$	0.20	0.2379
$V_2$	.05	.6915
$V_3$	.05	-1.1920
$V_4$	.60	.6000
$V_5$	.20	1.3260
$V_6$	.05	-2.8710
$V_7$	.05	1.7480
$V_8$	.60	.6000
Objective function mass, lb . . . .	10 829	9377
Number of violated constraints . . .	94	0

TABLE III.- FUNCTIONS OF EAL PROCESSORS

Processor name	Function
TAB	Creates data sets containing tables of joint locations, section properties, material constants, etc.
ELD	Defines the finite-element connections in model
E	Generates sets of information for each element, including connected joint numbers, geometrical data, material, and section property data
EKS	Adds the stiffness and stress matrices for each element to the set of information produced by the E processor
SEQ	Determines joint sequences, i.e., equation numbering sequences to be used in sparse matrix solution methods
TAN	Analyzes element interconnections and topology and creates data sets used to assemble and factor the system mass and stiffness matrices
K	Assembles the unconstrained system stiffness matrix in a sparse matrix format
M	Assembles the unconstrained system mass matrix in a sparse matrix format
KG	Assembles the unconstrained system initial-stress (geometric stiffness) matrix in a sparse matrix format
RSI	Factors the assembled system matrices
DRSI	Similar to RSI, factors double precision SPAR format matrices
EQNF	Computes equivalent joint loading associated with thermal, dislocational, and pressure loading
SSOL	Computes displacements and reactions due to applied loading at the joints
LSK	Forms partial or complete system stiffness (K) and damping (D) matrices in a sparse matrix form called LS format
LSU	Translates arbitrary source K and M data into LS or SPAR format and transforms SPAR and LS format matrices
GSF	Generates element stresses and internal loads
PSF	Prints the information generated by the GSF processor
ES	Analyzes element interior state, given joint displacements, and initial strains, if present; creates and stores stresses and internal load data

TABLE III.- Concluded

Processor name	Function
EIG	Solves linear vibration and bifurcation buckling eigenproblems
E4	Similar to EIG
SYN	Produces mass and stiffness matrices for systems comprised of interconnected substructures
STRP	Computes eigenvalues and eigenvectors of substructured systems
SSBT	Back-transforms synthesized system results into individual substructure terms used in conjunction with SYN and STRP
AUS	Performs matrix arithmetic functions and is used in construction, editing, and modification of data sets
DCU	Performs data management functions including display of table of contents, data transfer between libraries, changing data set names, printing data sets, and transferring data between libraries and sequential files
VPRT	Performs editing and printing of data sets that are in the form of vectors on the data libraries
PLTA } PLTB } PXY }	Produce graphic displays of finite-element models and computed results such as vibration and buckling modes, stresses, and response histories
PR	Generates reports of dynamic response analysis
DR	Computes linear transient modal response and back-transforms to determine any required system response details and maximum-minimum and time-of-occurrence data
U1	Creates, edits, and manipulates runstreams and permits direct table input
U3/RP2	Produces tabular multipage reports, using formats, headings, and footnotes prescribed by the user at execution time
U4/VU	Enables vector arithmetic functions
FSM	Creates SPAR-format matrices for compressible fluid elements
PS	Prints SPAR-format matrices and factored system matrices produced by RSI or DRSI
EI1	Utility processor that operates on element state information
PRTE	Prints contents of the element state

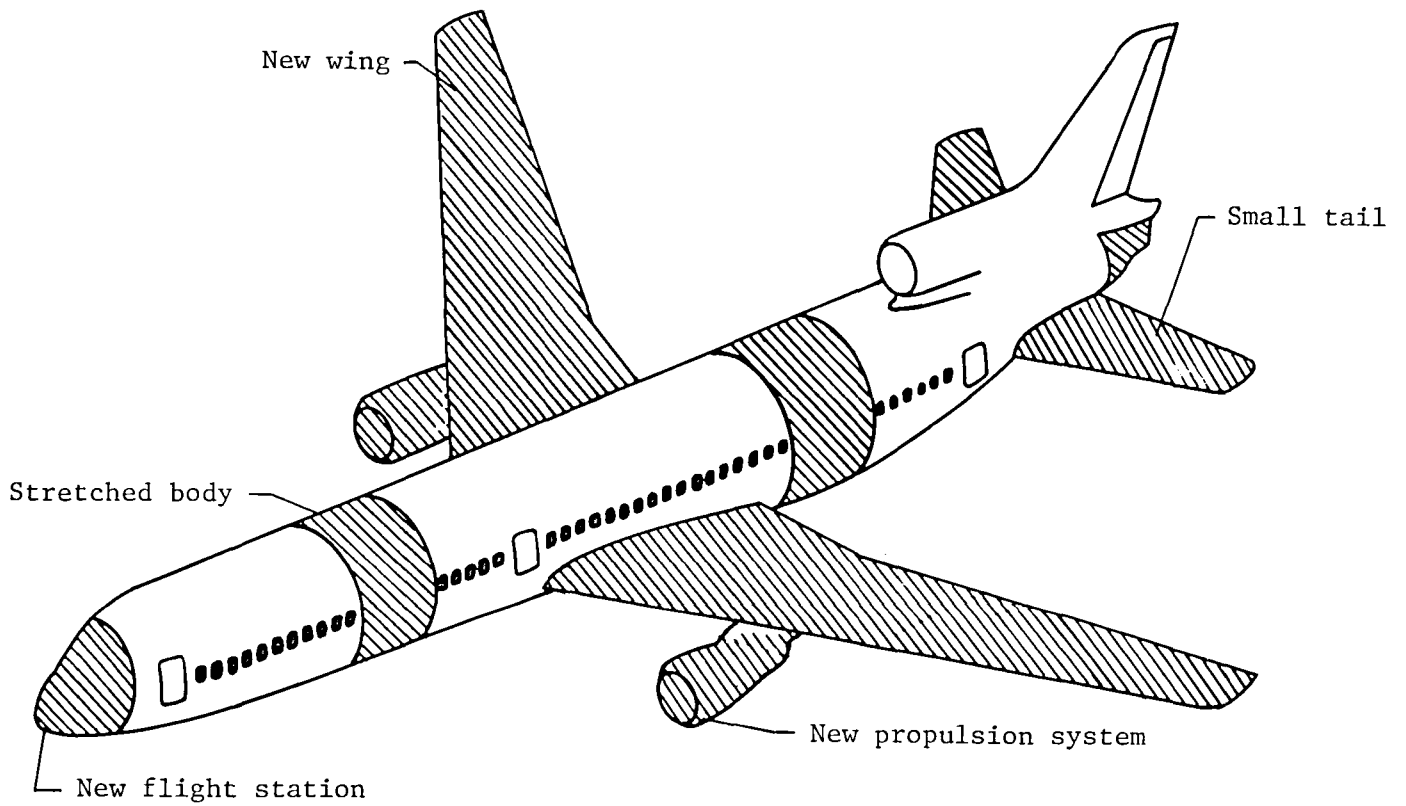
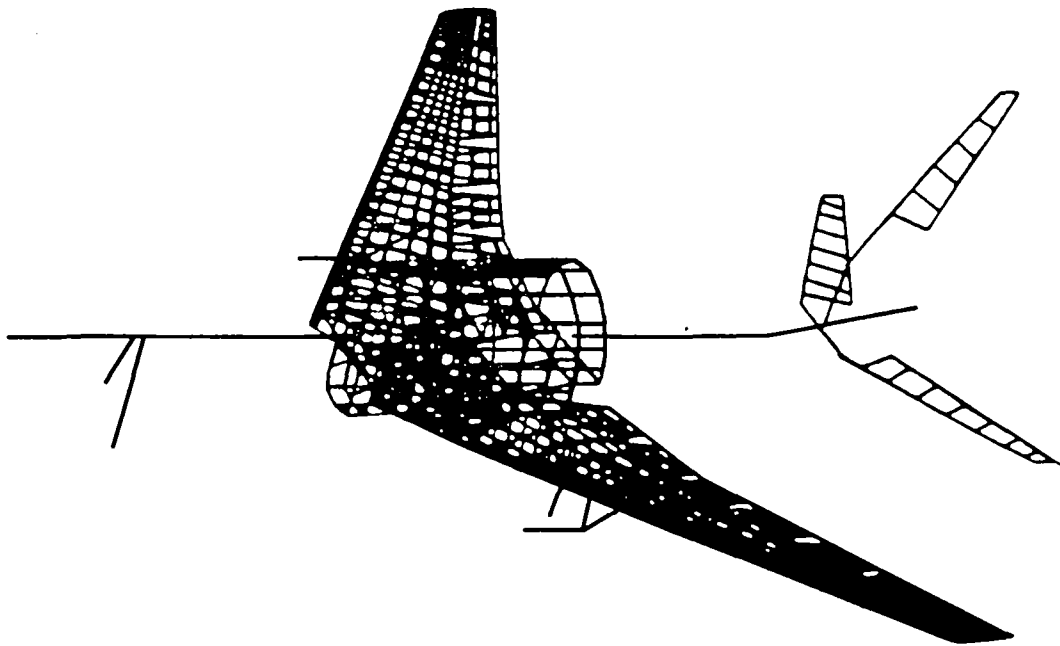
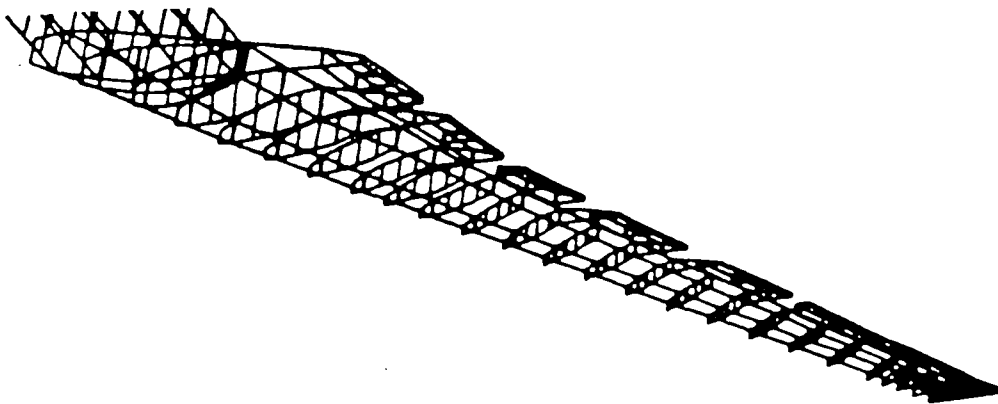


Figure 1.- L-1011 derivative advanced transport airplane. Modifications are indicated by shaded regions.



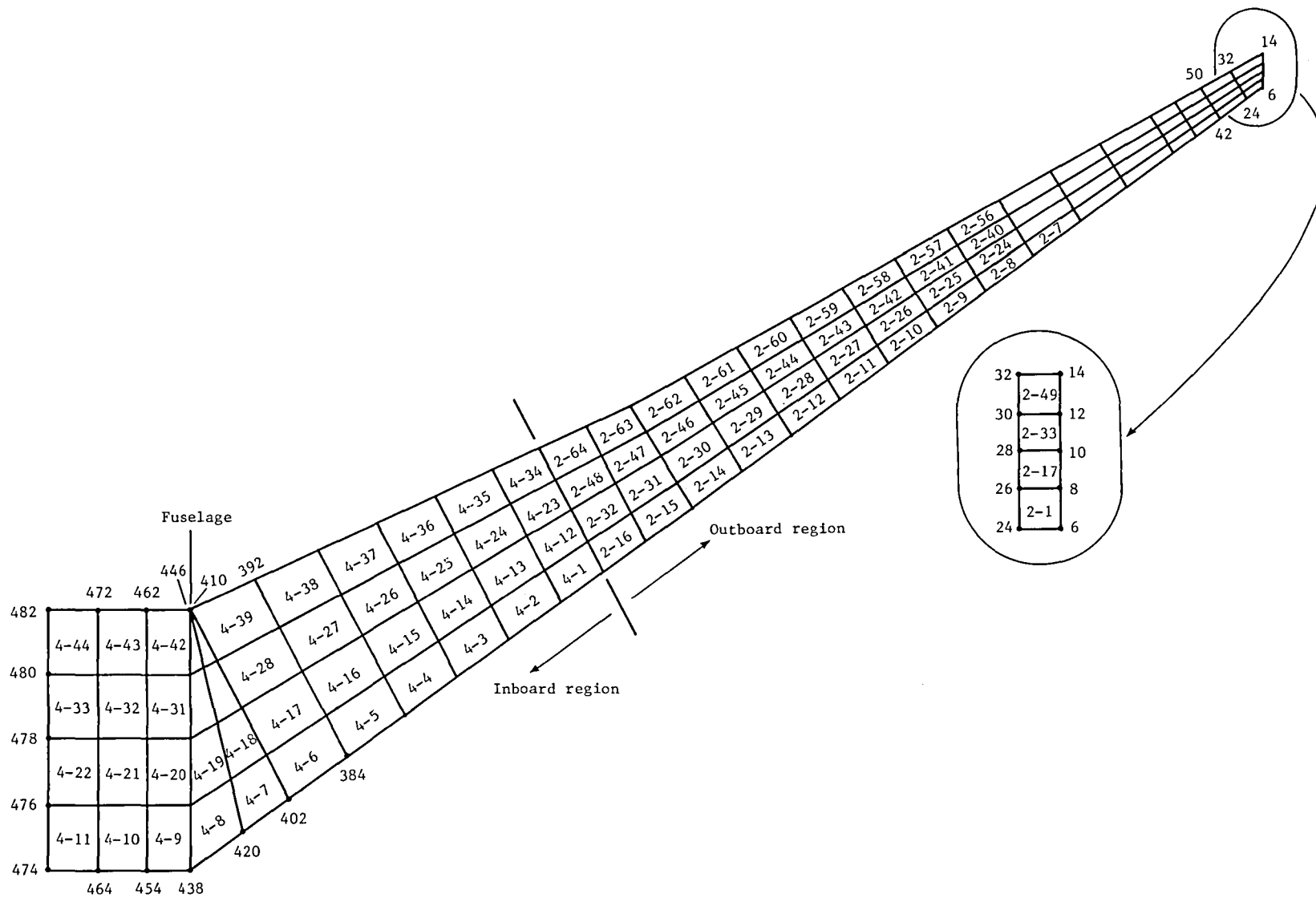
(a) Overall model.



(b) Model of wing.

Figure 2.- Finite-element structural model.





(b) Lower wing surface.

Figure 3.- Concluded.

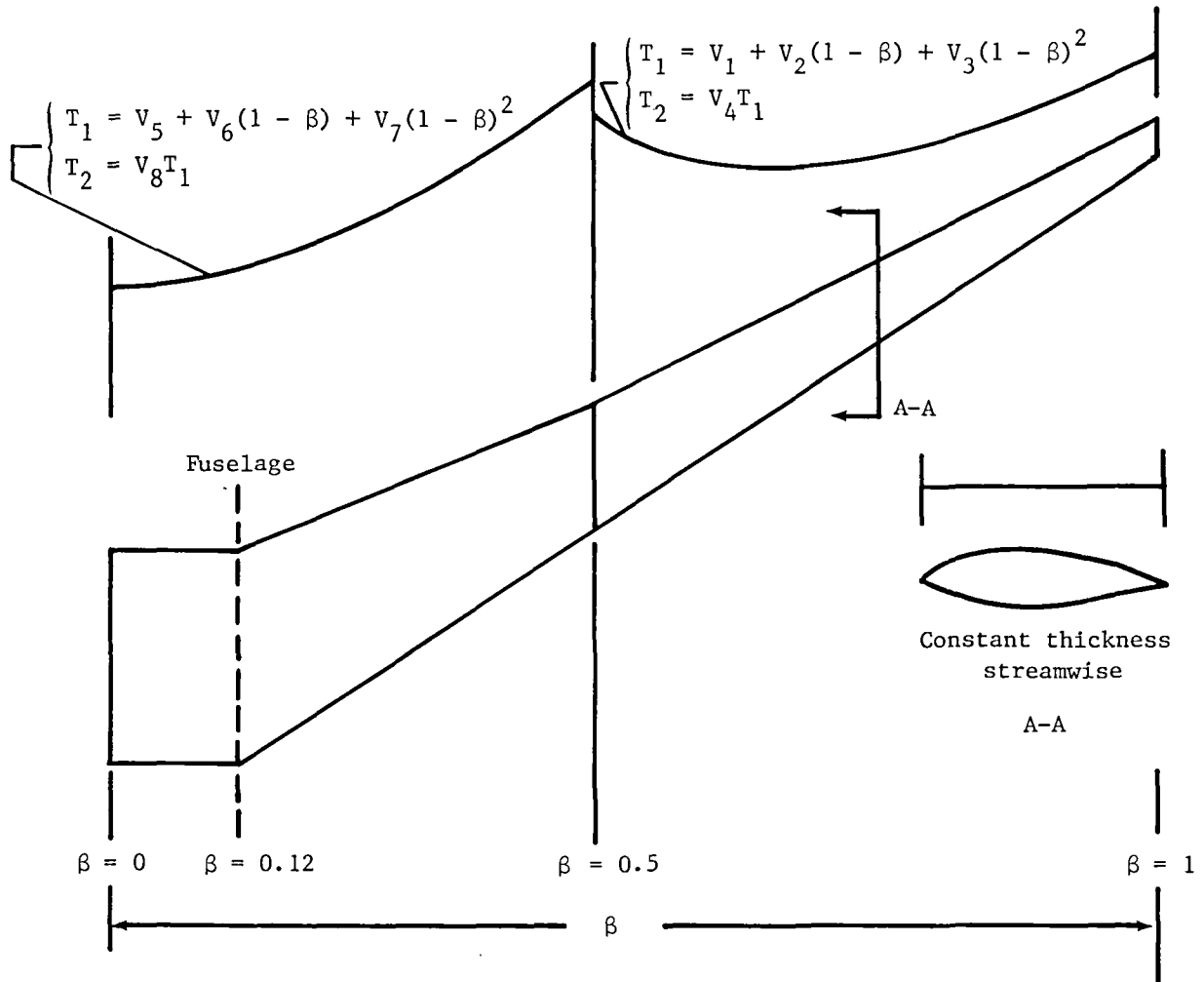


Figure 4.- Thickness distributions for wing cover panel.

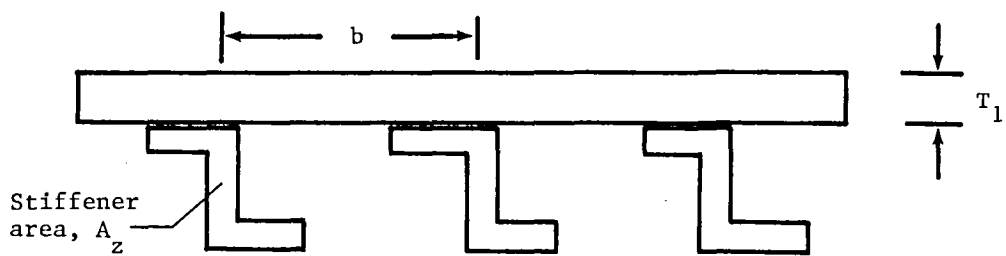


Figure 5.- Schematic drawing of stiffener and skin.  $A_z = T_2/b$ , where  $T_2$  is the smeared thickness of the stiffener.

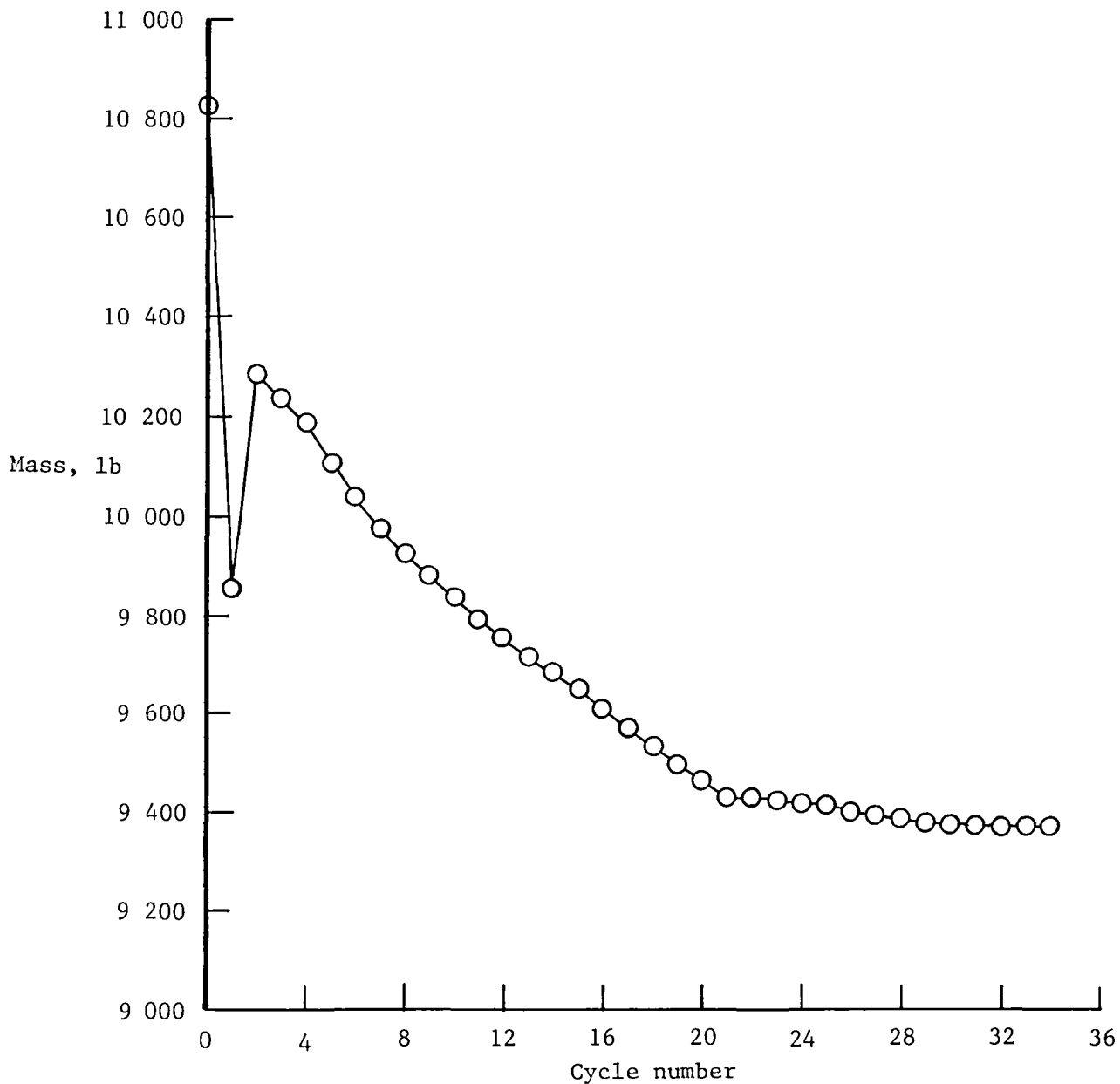


Figure 6.- Mass history of sized cover panels.



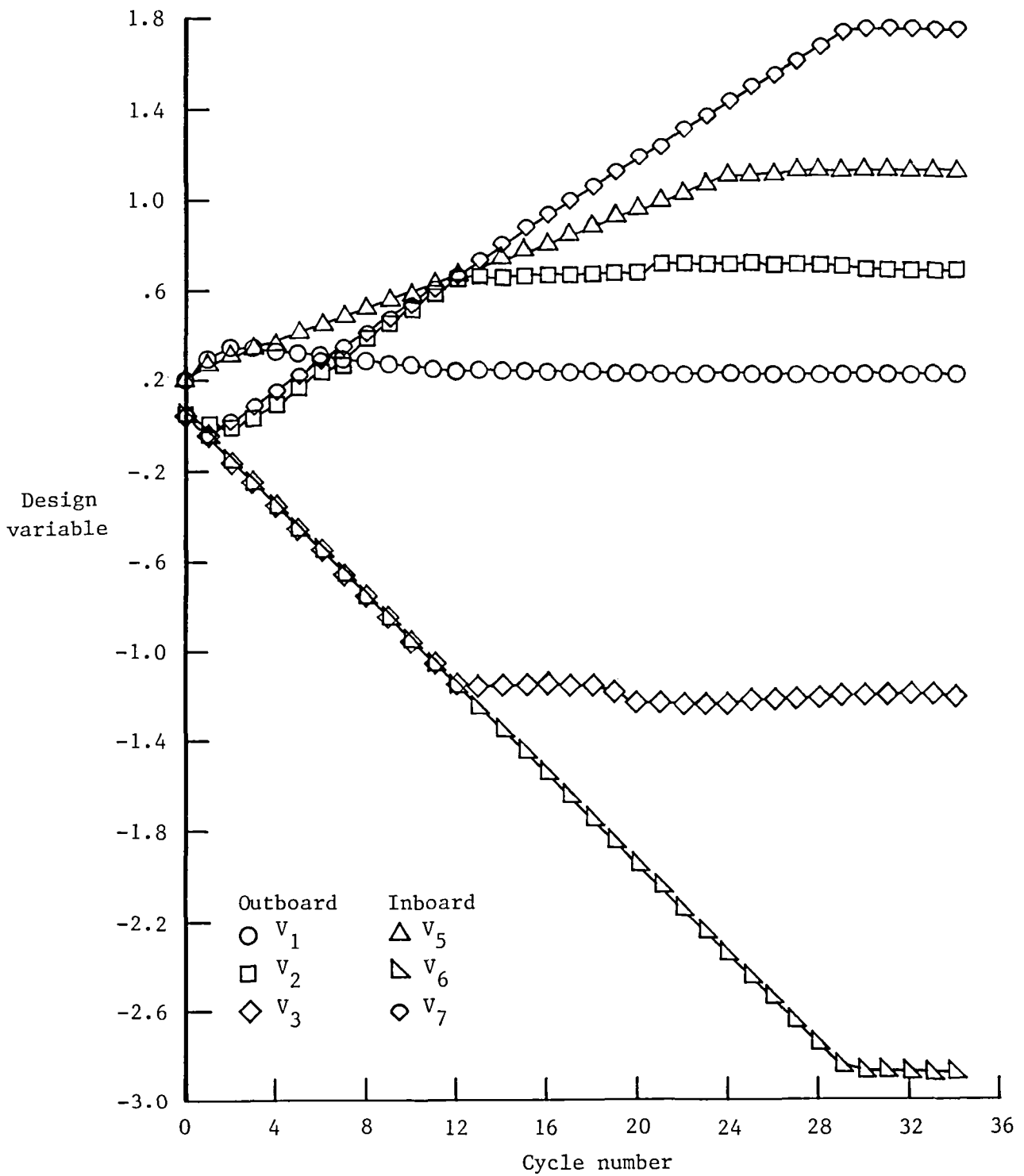
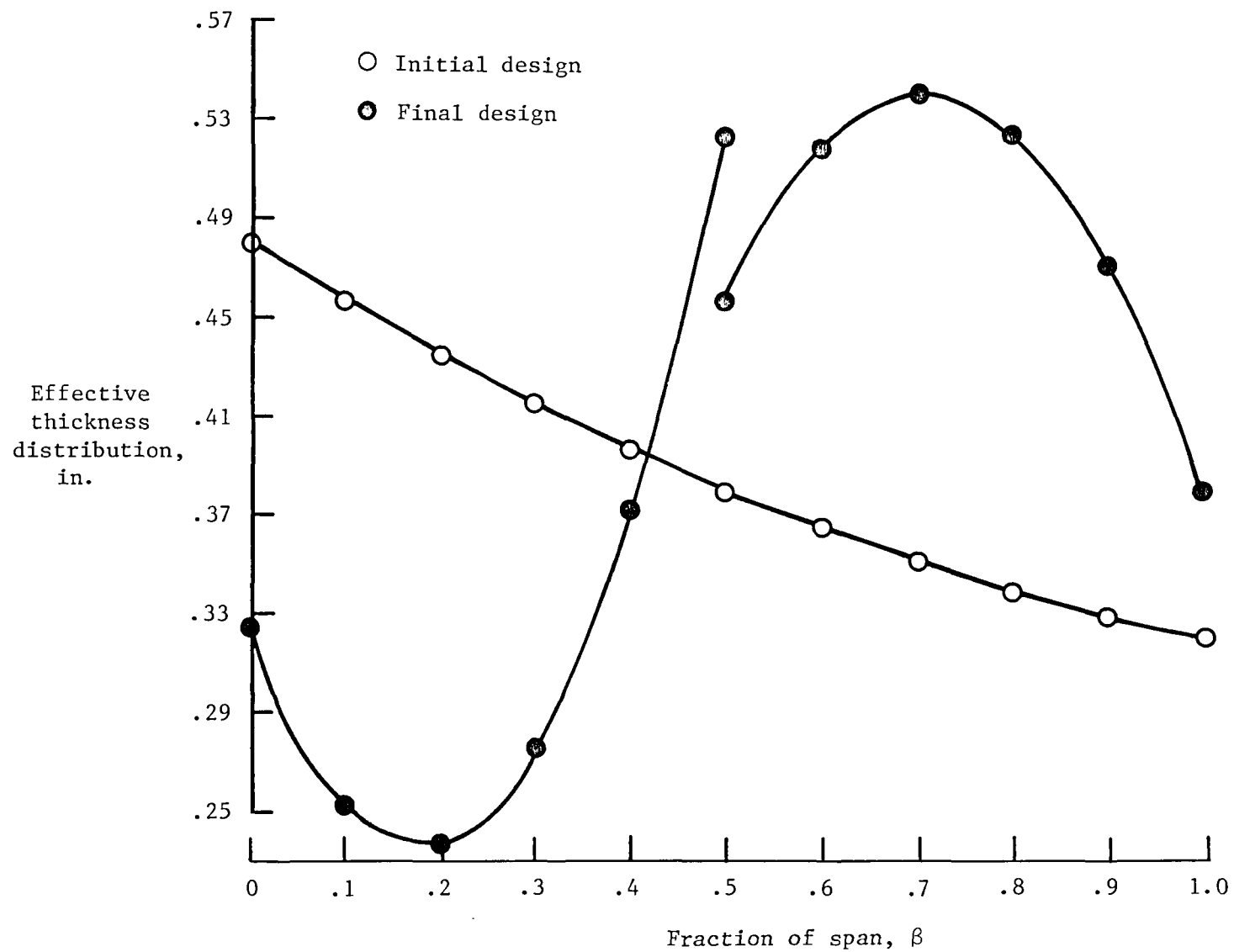
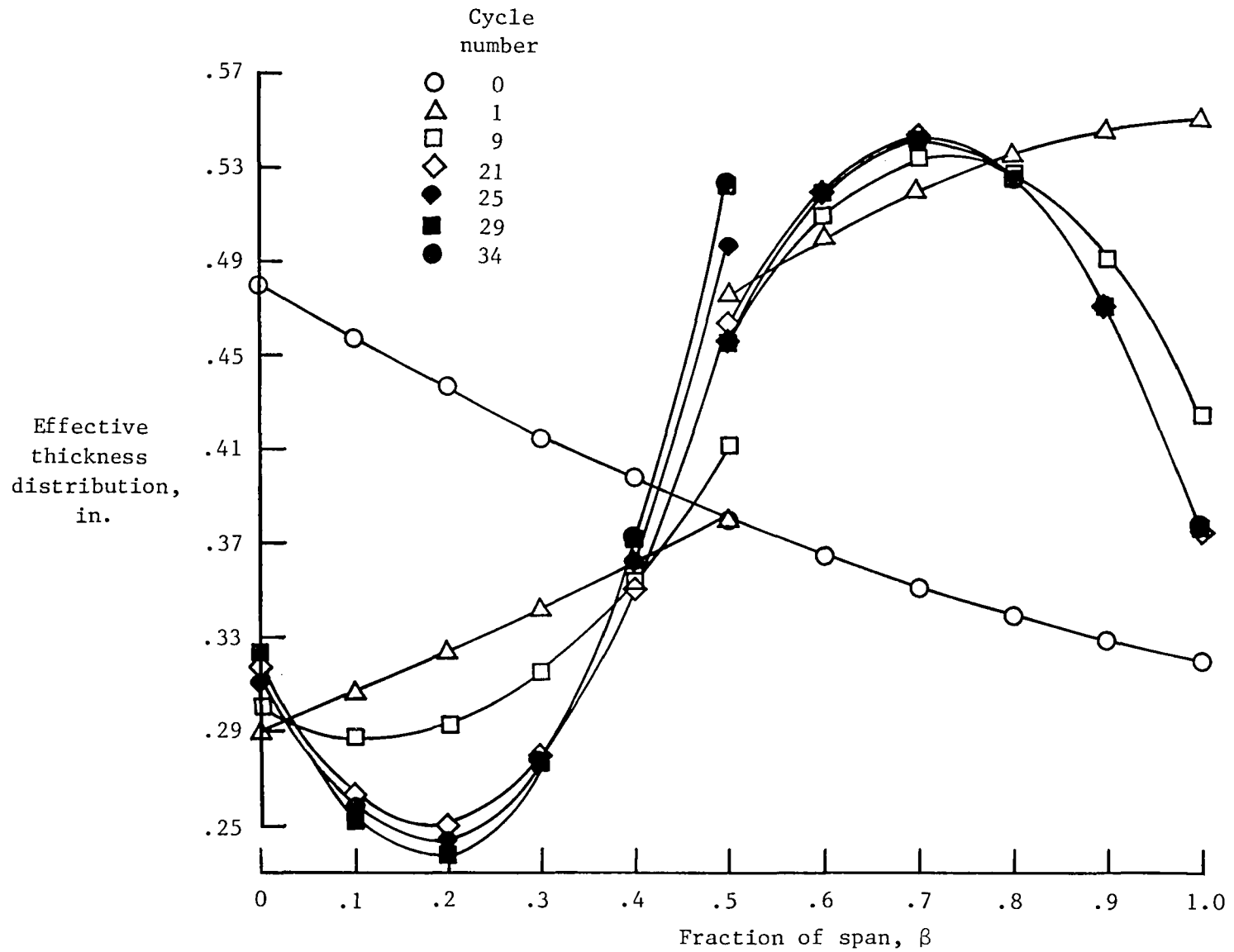


Figure 7.- Design variable history.



(a) Initial and final design.

Figure 8.- Effective spanwise thickness.



(b) Various design cycles.

Figure 8.- Concluded.

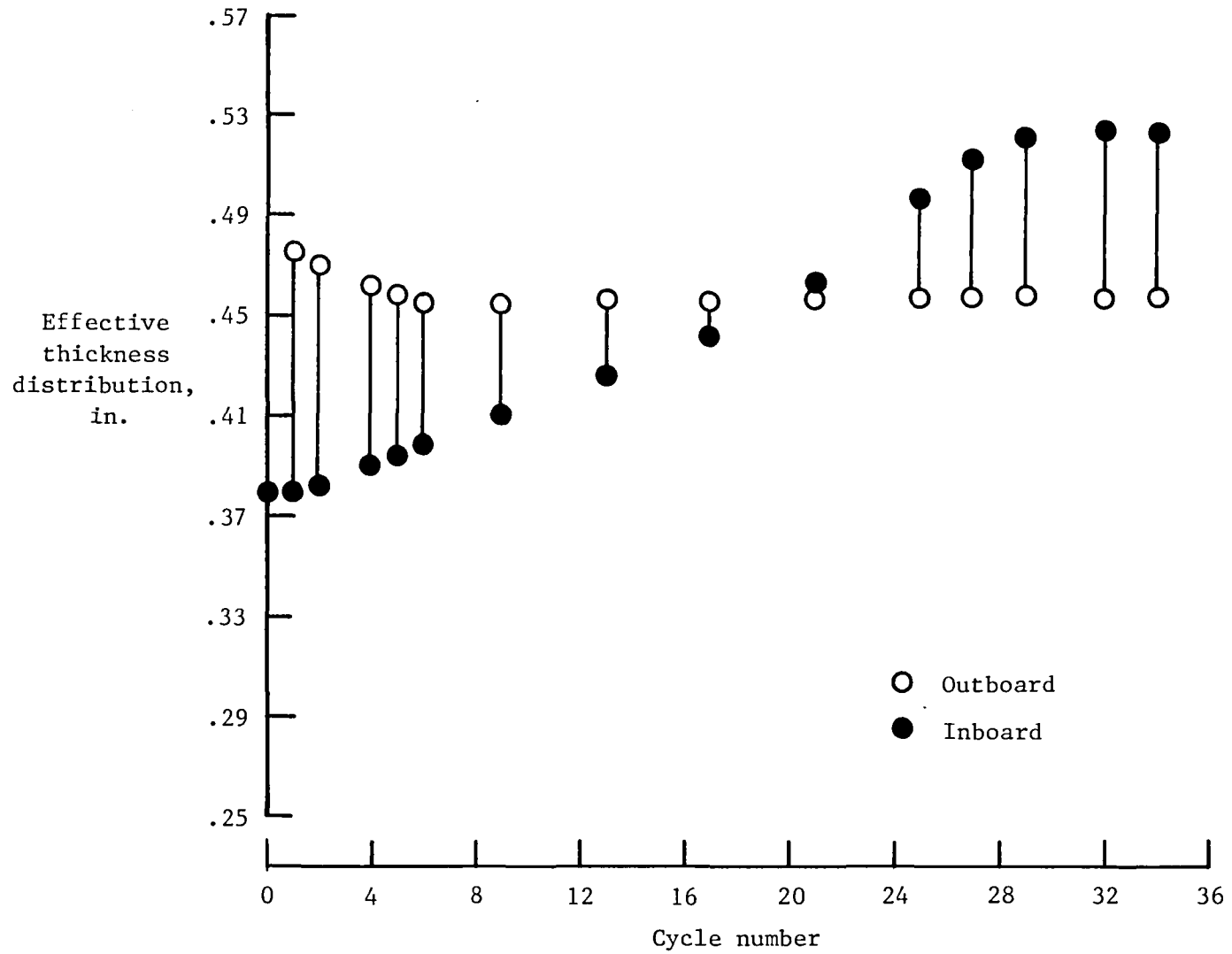


Figure 9.- Skin thickness gap at 50-percent span location.

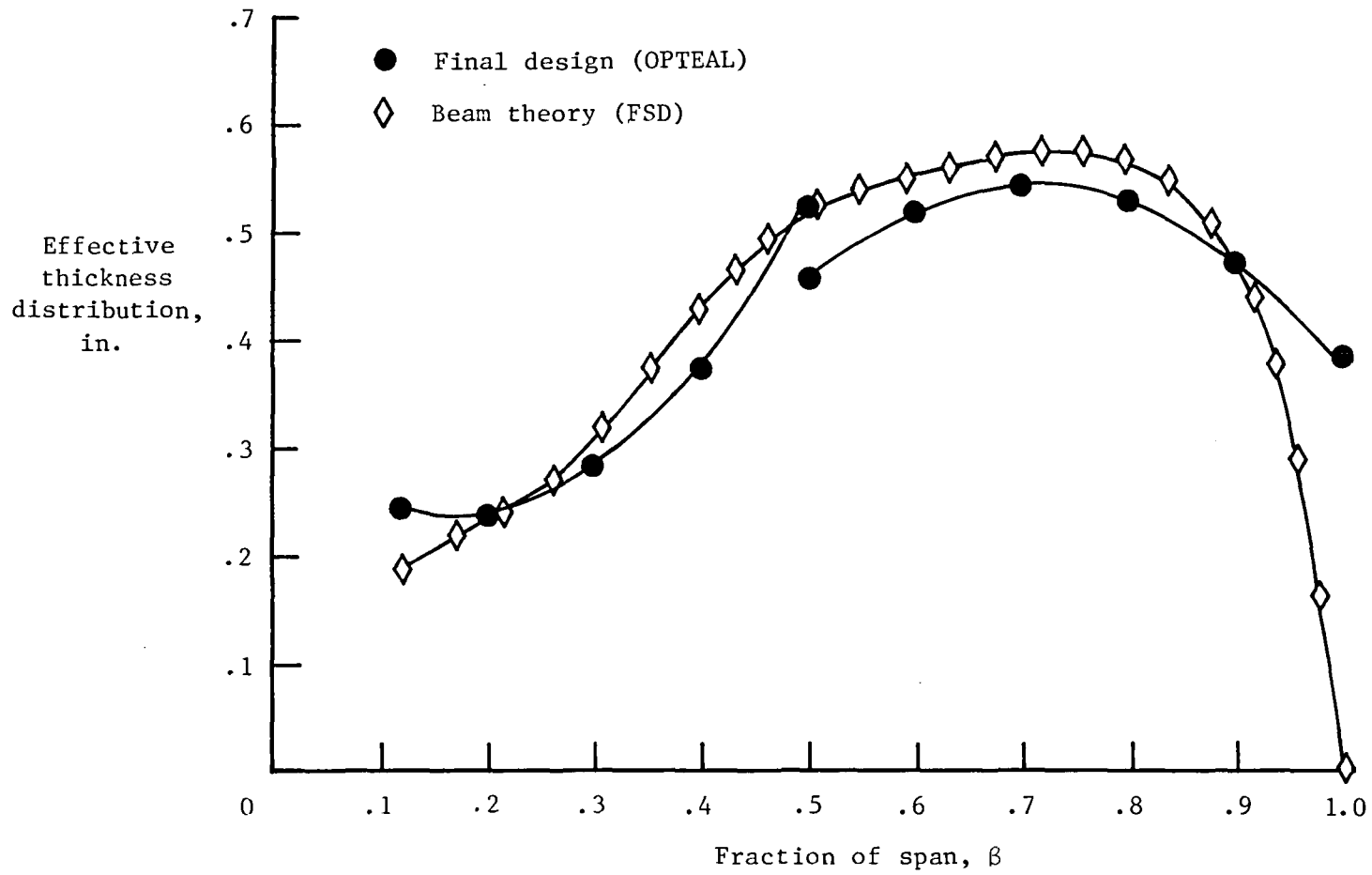
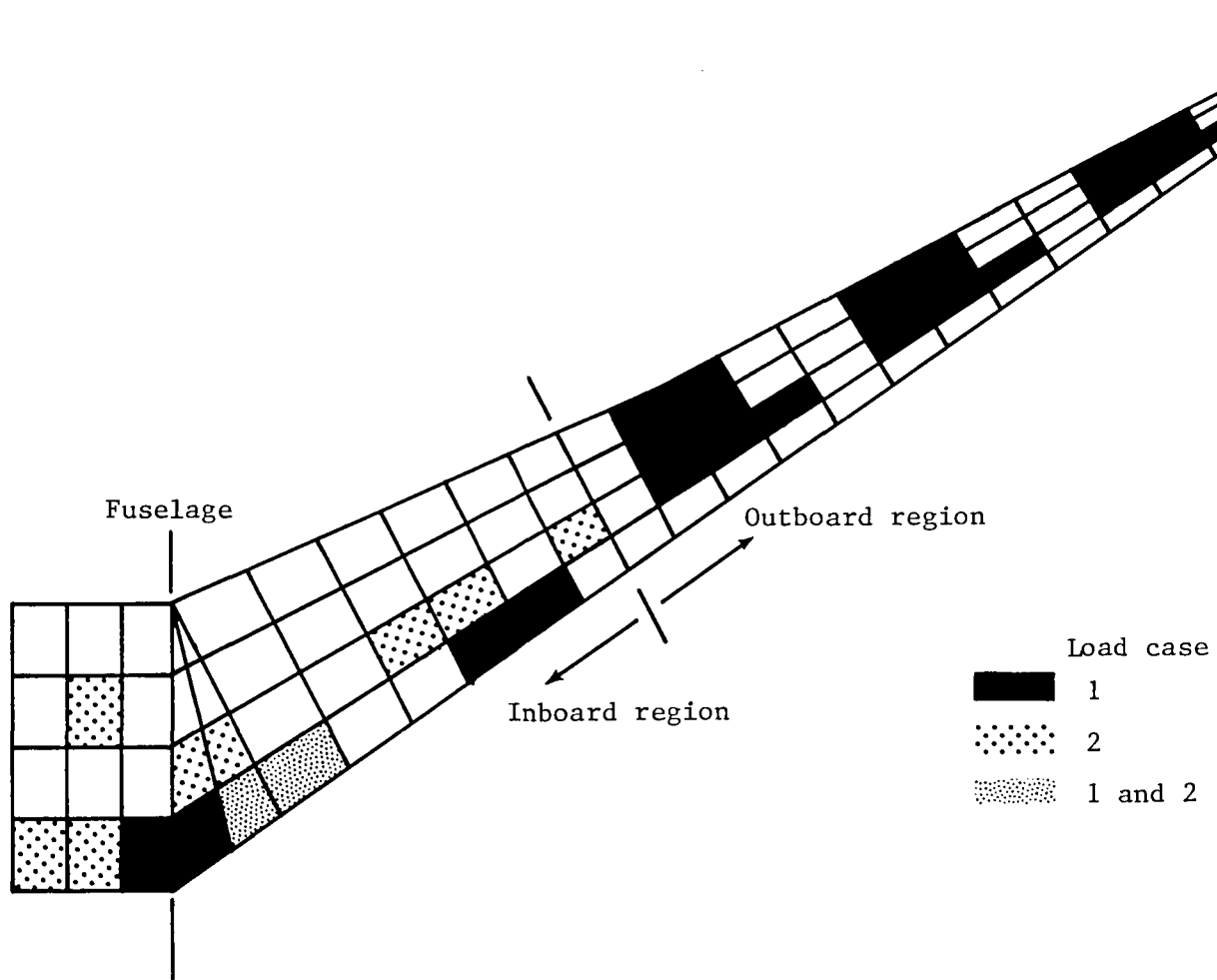
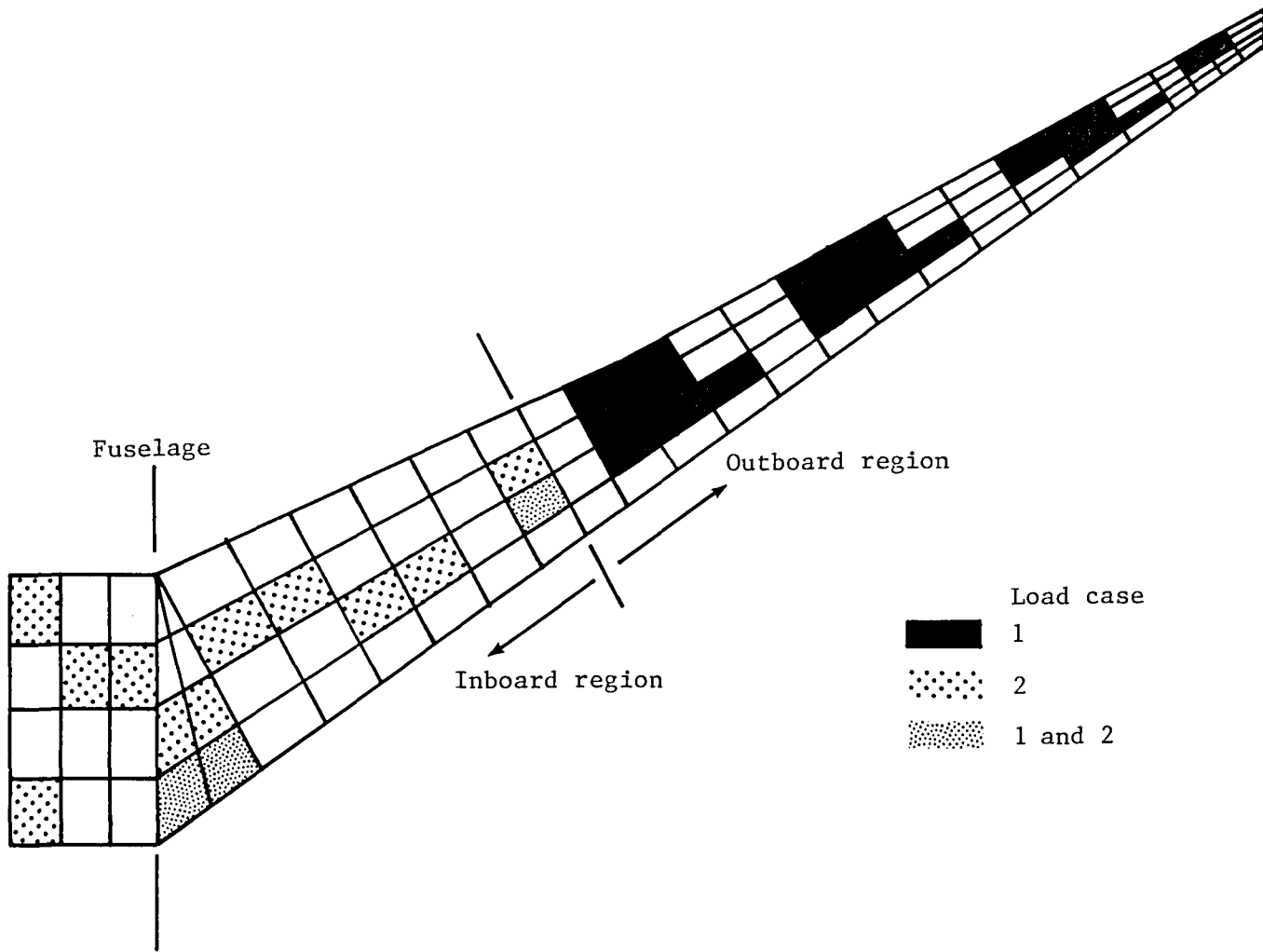


Figure 10.- Thickness distribution in wing.



(a) Upper wing surface.

Figure 11.- Distribution of fully stressed skin elements in sized cover panels of optimized wing.



(b) Lower wing surface.

Figure 11.- Concluded.

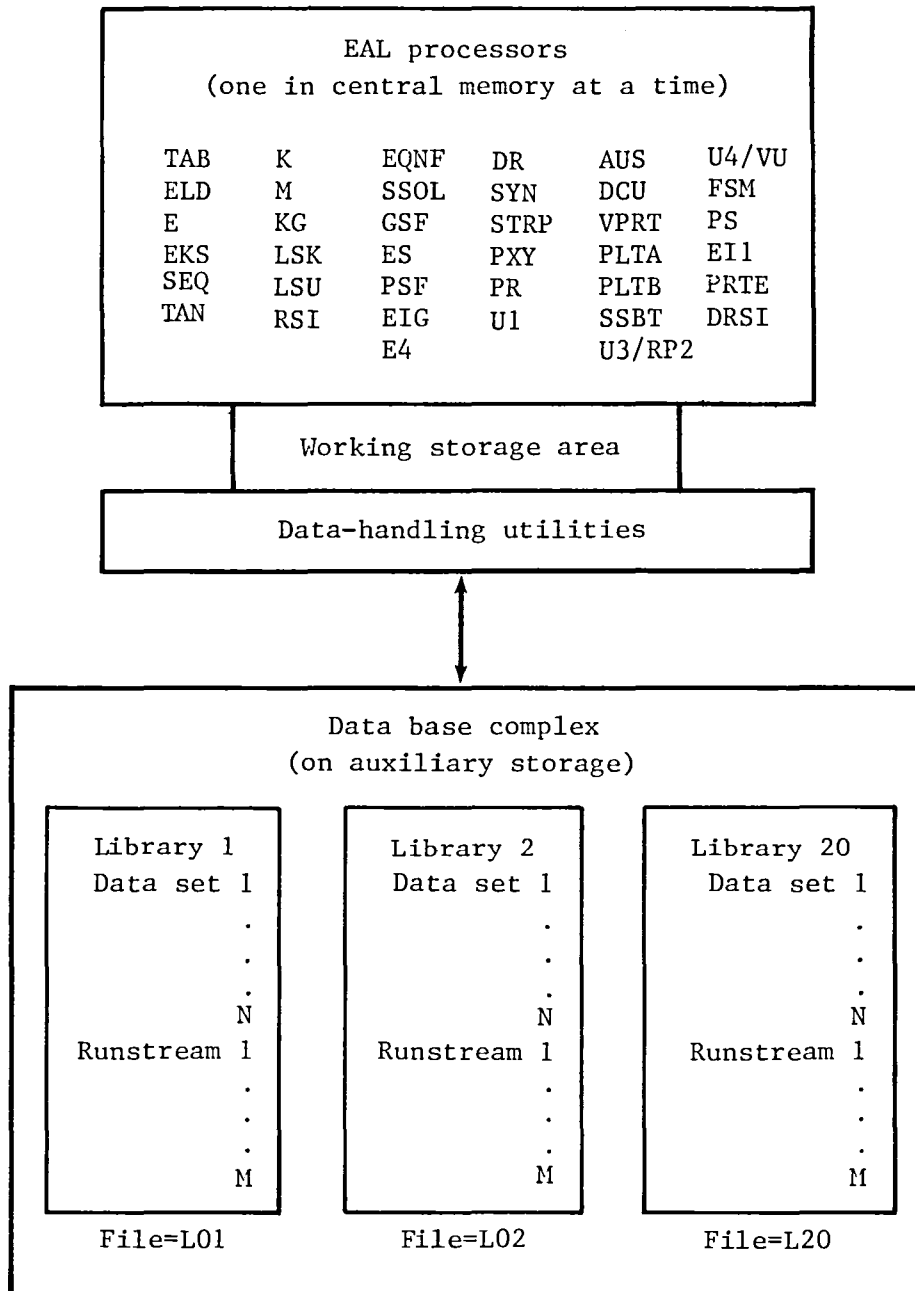


Figure 12.- Schematic of EAL system configuration.

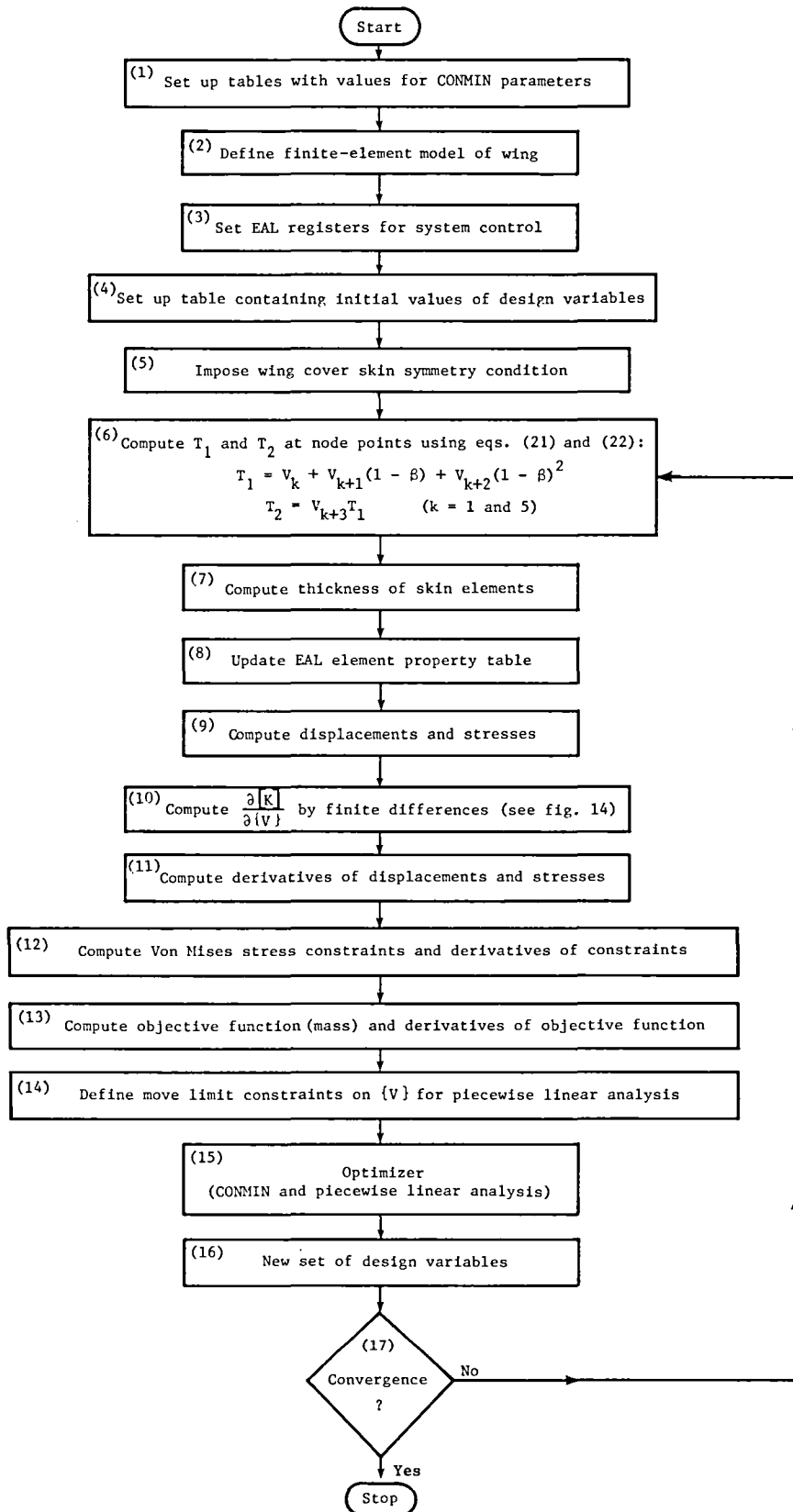


Figure 13.- OPTeAL block diagram.

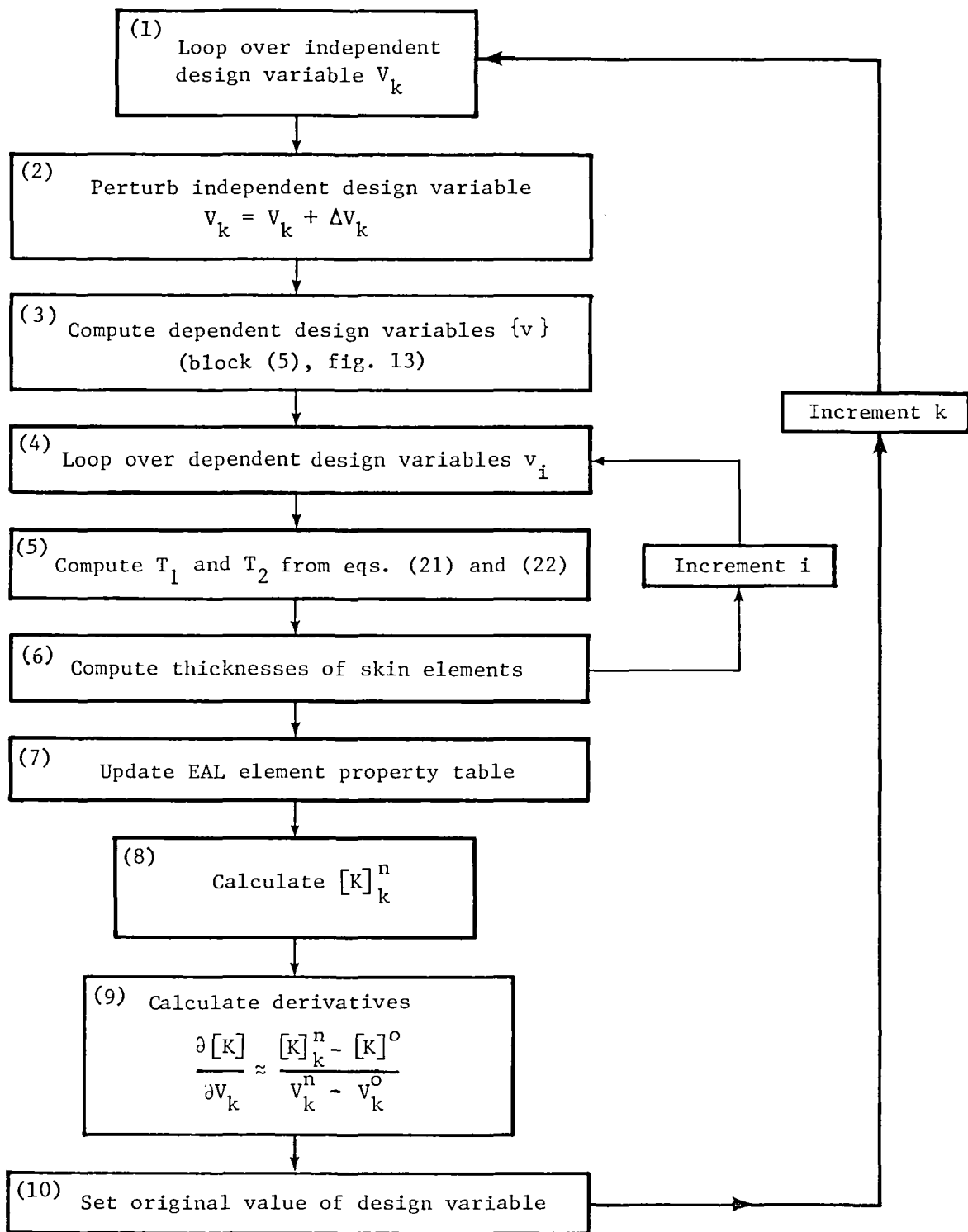


Figure 14.- Detailed description of block (10) in figure 13 for stiffness matrix derivative.



1. Report No. NASA TM-87597		2. Government Accession No.		3. Recipient's Catalog No.	
4. Title and Subtitle Application of Mathematical Optimization Procedures to a Structural Model of a Large Finite-Element Wing				5. Report Date January 1986	
				6. Performing Organization Code 506-53-53-07	
7. Author(s) Joanne L. Walsh				8. Performing Organization Report No. L-15930	
9. Performing Organization Name and Address NASA Langley Research Center Hampton, VA 23665-5225				10. Work Unit No.	
				11. Contract or Grant No.	
				13. Type of Report and Period Covered Technical Memorandum	
12. Sponsoring Agency Name and Address National Aeronautics and Space Administration Washington, DC 20546-0001				14. Sponsoring Agency Code	
15. Supplementary Notes					
16. Abstract  An optimization system is described that consists of the finite-element analysis program known as Engineering Analysis Language (EAL), the CONMIN optimization program, and a piecewise linear analysis. The optimization analysis system (OPTEAL) is used to minimize the mass of a transport wing subject to stress constraints for two static load conditions. The purpose of this paper is to describe the optimization procedure and the optimization analysis system (OPTEAL) and to compare the optimized results with fully stressed design results.					
17. Key Words (Suggested by Author(s)) Structural sensitivity analysis Structural optimization Finite-element method Engineering Analysis Language (EAL)			18. Distribution Statement Unclassified - Unlimited  Subject Category 39		
19. Security Classif. (of this report) Unclassified		20. Security Classif. (of this page) Unclassified		21. No. of Pages 41	22. Price A03



**National Aeronautics and  
Space Administration  
Code NIT-4**

**Washington, D.C.  
20546-0001**

Official Business  
Penalty for Private Use, \$300

**BULK RATE  
POSTAGE & FEES PAID  
NASA Washington, DC  
Permit No. G-27**

**NASA**

**POSTMASTER: If Undeliverable (Section 158  
Postal Manual) Do Not Return**

---